STUDY OF MECHANICAL CHARACTERISTICS OF WELDED JOINTS OF DISSIMILAR AUSTENITIC STEELS SS 202 AND SS 304 BY COLD METAL TRANSFER WELDING PROCESS

A Thesis Submitted

In partial fulfillment for the award of the degree of

Master of technology

In

Production Engineering

SUBMITTED BY

Prateek Raj
(2K18/PIE/08)

UNDER THE GUIDANCE OF

Dr N. Yuvaraj
Assistant Professor

DEPARTMENT OF MECHANICAL, PRODUCTION & INDUSTRIAL AND AUTOMOBILE ENGINEERING
DELHI TECHNOLOGICAL UNIVERSITY
BAWANA ROAD, DELHI-110042
AUGUST 2020

CANDIDATE'S DECLARATION

I, PRATEEK RAJ, hereby certify that the work which is being presented in this thesis entitled "**STUDY OF MECHANICAL CHARACTERISTICS OF WELDED JOINTS OF DISSIMILAR AUSTENITIC STEELS SS 202 AND SS 304 BY COLD METAL TRANSFER WELDING PROCESS**" being submitted by me is an authentic record of my own work carried out under the supervision of **Dr. N. Yuvaraj, Assistant Professor, Department of Mechanical Engineering, Delhi Technological University, Delhi.**

The matter presented in this thesis has not been submitted in any other University/Institute for the award of M.Tech Degree.

PRATEEK RAJ

(2K18/PIE/08)

CERTIFICATE

I, PRATEEK RAJ, hereby certify that the work which is being presented in this thesis entitled "**STUDY OF MECHANICAL CHARACTERISTICS OF WELDED JOINTS OF DISSIMILAR AUSTENITIC STEELS SS 202 AND SS 304 BY COLD METAL TRANSFER WELDING PROCESS**" in the partial fulfillment of requirement for the award of degree of **Masters of Technology in Production Engineering** submitted in the **Department of Mechanical Engineering** at **Delhi College Of Engineering**, **Delhi University**, is an authentic record of my own work carried out during a period from July 2019 to July 2020, under the supervision of **Dr. N. YUVARAJ, Assistant Professor, Department of Mechanical Engineering, Delhi College of Engineering, Delhi.**

The matter presented in this thesis has not been submitted in any other University/Institute for the award of M.Tech Degree.

Dr N. Yuvaraj
Assistant Professor
Department of mechanical Engineering
Delhi Technological University, Delhi

ACKNOWLEDGEMENT

It is a matter of great pleasure for me to present my dissertation report on "**STUDY OF MECHANICAL CHARACTERISTICS OF WELDED JOINTS OF DISSIMILAR AUSTENITIC STEELS SS 202 AND SS 304 BY COLD METAL TRANSFER WELDING PROCESS**". First and foremost, I am profoundly grateful to my guide **Dr. N. YUVARAJ, Assistant Professor, Mechanical Engineering Department** for his expert guidance and continuous encouragement during all stages of thesis. I feel lucky to get an opportunity to work with him. Not only understanding the subject, but also interpreting the results drawn thereon from the graphs was very thought provoking. I am thankful to the kindness and generosity shown by him towards me, as it helped me morally complete the project before actually starting it.

I would like to extend my gratitude to **Prof. Vipin, Head, Mechanical Engineering Department** for providing this opportunity to carry out the present thesis work.

Finally and most importantly, I would like to thank **my family members** for their help, encouragement and prayers through all these months. I dedicate my work to them.

DATE:

PLACE:

PRATEEK RAJ

(2K18/PIE/08)

ABSTRACT

Welded joints of dissimilar stainless steel sheets have many industrial applications due to their cost effectiveness, light-weight, and high efficiency. Thin austenitic stainless steel sheets of different thicknesses are extensively used in the automation industry. Conventional welding techniques due to their high heat input and high spatters have always posed problems such as burn-through and distortion for welding these joints of thin austenitic steels. The CMT welding technique is effectively used for the joining of thin sheets due to its characteristics of lower distortion rate and low heat input. In this research work, austenitic stainless steels of grade SS 202 and SS 304 of thickness 1.2 mm and 2 mm respectively were welded by CMT welding technique and studied the mechanical characteristics of dissimilar stainless steel joints. Taguchi L9 optimization technique was used to find the optimized process variables for obtaining the maximum tensile strength. The maximum tensile strength of dissimilar joint welded at 115 A current, 4 mm/s welding speed, and 10% arc length correction factor was found to be 291 MPa. The maximum micro-hardness value of the weld zone was achieved and the lower value was observed in the heat-affected zone (HAZ). The X-ray diffraction (XRD) technique was utilized to detect the residual stresses of the welded joint. The residual stress was observed in compressive nature in the weld zone and base plate and of tensile nature in the heat-affected zone (HAZ). CMT welding process can produce high strength dissimilar austenitic steel joints of different thicknesses.

Keywords: CMT; SS 202/304; Tensile Strength; Hardness; Residual stresses

CONTENTS

LIST OF FIGURES

LIST OF TABLES

CHAPTER 1: INTRODUCTION

Fusion welding is considered as one of the most important and best technology to enhance sustainable manufacturing amongst the numerous manufacturing technologies. Any product is very difficult to manufacture without using the process of joining due to technological limitations. Several components of the products are typically assembled and fusion practices mostly help to fabricate and rise process proficiency [Tseng et.al. (2014)]. Joining different metals is preferred as it helps in giving benefits of various materials that offer distinctive solutions to different engineering requirements [Taban et.al. (2010)]. A reduction in weight and cost of the product without hindering the structural requirements and safety is one of the basic advantages of fusing different materials

There are many joining processes for dissimilar materials that have received remarkable consideration in recent years. The dissimilar fusion weld must acquire satisfactory tensile and ductility test results so that the joint will be successful within the weld [Ghosh et.al. (2017)]. There are several engineering-related applications like automobile fabrication, power plants, boilers, railways, aerospace industries ,etc where dissimilar metal joints are used [Ghosh et.al. (2017) and Chaudhari et.al. (2014)]. Therefore joining of dissimilar metals is highly considered in recent years.

Different welding operation which includes fusion joining of dissimilar materials till now is Gas metal arc welding (GMAW), Metal Inert gas welding (MIG), Shielded metal arc welding (SMAW), Pressure Welding, Brazing, Soldering, etc. The major challenge in these fusion welding processes of dissimilar metals is large heat-affected zones and selection of filler material. The large heat affected zone produces regions of brittle intermetallic compounds which may result in a fracture. Thus HAZ is mostly the region of fracture. Also selecting suitable filler material is most important as it controls the mechanical properties and microstructure characterization in the weld zone.

Amongst the numerous process mentioned above, GMAW/MIG is the most used process for joining ferrous and non-ferrous metals due to its supreme weldment characteristics [Ibrahim et.al. (2012)]. Apart from the gap bridging expertise, GMAW is also a specialized technique that covers up easily the loss of the alloys made during welding [Hu et.al. (2016)]. This method is

especially preferred in applications related to the automotive industry. Anyhow, with the recent shift of these industries towards environmental sustainability and safety of passengers, different grades of steel are now being used for fabrications. Thin sheet alloys have a high coefficient of thermal conductivity and thermal expansion and so they pose some problems like burn through and distortion during arc welding. Welding dissimilar materials of different thicknesses have always been problematic when done by a conventional welding process due to high heat input and high spatters. Controlled heat input is an essential condition to avoid such problems [Tseng et.al. (2014) and Gungor et.al. (2014)]. Thus a need for a welding technique arises which can be used to join thin sheets and eradicate these problems. CMT techniques lessen these difficulties to a great extent. Properties like narrow HAZ improved productivity and narrow distortion makes cold metal transfer welding (CMT) technique preferable for joining thin plates when compared to other processes [Ghosh et.al. (2017)].

Cold Metal Transfer (CMT) is a newly introduced method of joining thin sheets on the basis of conventional short-circuiting (CSC) technique established via "Fronius of Austria". It is a technological up gradation of Gas Metal Arc Welding (GMAW) process and is highly superior to GMAW in terms of spatter, distortion, burn through and welding cost due to its unique feature known as low heat input. It also provides high gap bridge-ability which is highly appropriate for automation. CMT welding is an automatic welding technique having a controlled deposition of material during the short-circuiting of the work-piece to an electrode and is well described for its working with a low heat input [Feng et.al. (2009)]. This results in less damage to the base metal, lower deformation, and residual stress. In a conventional arc welding process, the filler wires move continuously in the outward direction till a short-circuit takes place. Whereas in a CMT process, the filler wire is both pushed as well as retracted during welding, and thus it is called an intelligent system. In this process, the movement of the feeding wire with an oscillating frequency up to 70 Hz is mostly used [Pickin et.al. (2011)].

1.1 Cold Metal Transfer Process

CMT is a diligent technique that offers deposition of material at a lower heat input with a digitally controlled wire feeding system [Pickin et.al. (2011)]. In this newly introduced welding process, as the arcing starts the electrode moves toward the weld puddle. As the electrode tip interacts with the molten metal in the weld pool, an arc gets extinguished. The value of current

reduces significantly to a non-zero value and this in a way circumvents the chances of spatter. The dropped welding current value results in a remarkable reduction in the thermal heat input. And thus this becomes the most favorable conditions and a feasible technique to weld thin sheets with no or very less distortion, a lower rate of dilution and lower stresses in the weld zone [Cao et.al. (2013), Cao et.al. (2014), Wang et.al. (2008), Lorenzin et.al. (2009) and Lin et.al. (2013)]. The motion of the wire reverses which is digitally controlled by a synergic power source which supports the weld drop detachment during short-circuiting [Yang et.al. (2013)]. The feed wire motion gets reversed thus repeating the whole process all over again [Gungor et.al. (2014)]. CMT process has become a well known reliable welding technique because of its low thermal heat input feature which results in a decrease in the heat-affected zone (HAZ). The period in which the deposition of a droplet from an electrode in this molten state weld pool takes place is called a CMT welding electrical cycle signal. The whole process from droplet detachment to energy distribution occurs in phases and involves a study of current and voltage waveforms.

Fig. 1. shows the current and voltage waveforms and the study of it is an essential condition for understanding the energy dissipation of different phases during the process of droplet transfer.

The three different phases in the CMT cycle are as follows:-

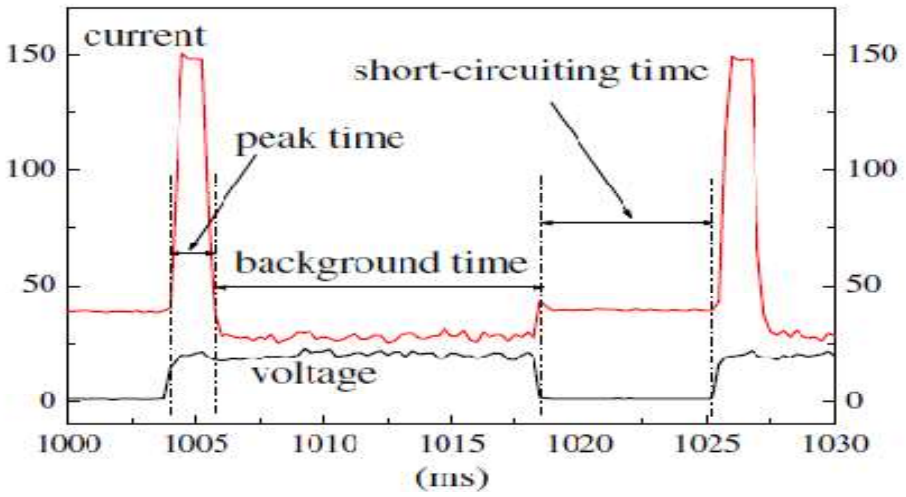

Fig. 1. Current and Voltage waveforms of CMT process [Feng et.al. (2009)]

I. **The Peak current phase**: It is a 'constant arc voltage' (CAV) corresponding to a high pulse of current for a short duration triggering the ignition of the welding arc effortlessly and then melts the electrode wire to form a droplet.

II. **The Background current phase**: This phase has corresponded to a lowered current value. As in the peak current phase, the liquid droplet is formed on the wire tip, the current is reduced to non-zero to prevent the globular transfer which helps in avoiding any spatter generation. This phase lasts until short-circuiting occurs.

III. **The Short-circuiting phase**: This phase corresponds to a zero arc voltage. In this, the arc voltage drops to zero as the wire comes in contact with the weld pool. At the same instance, the retractor mechanism supplied to the wire feeder by 'Digital Process Control' (DPC) which provides the wire with a back-drawing effort assists in the liquid bridge fracture and transfer of material into the weld pool. The arc is then re-ignited and then the sequence repeats itself all over again [Feng et.al. (2009)].

The welding current and the reverse feeding of filler electrode wire have a complex waveform which mechanically enforces the metal movement making it hard to acknowledge the relationship existing between the welding parameters, the metal, and the heat transfer. But by maintaining perfect management of arc duration and higher edge tolerance a CMT welding process becomes a perfect technique for industrial applications thus overcoming the challenges of other conventional welding techniques.

A CMT arc welding can be demonstrated in the following steps as shown in Fig. 2.

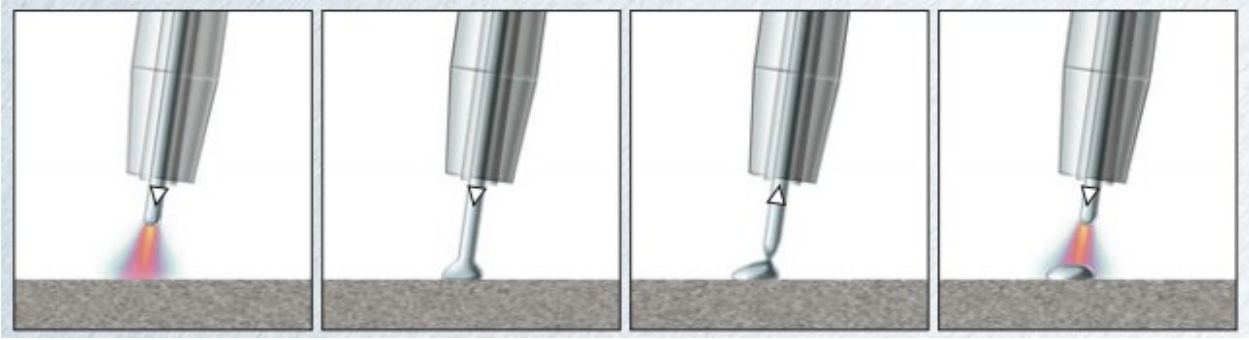

(a) (b) (c) (d)

Fig. 2. Demonstration of CMT welding arc [Merkler M. (2004)]

a) During arcing the molten metal on the electrode tip moves towards the weld pool.
b) The arc is extinguished the moment the filler electrode wire is dipped in the weld pool. The current value gets lowered.
c) The backward movement of filler wire assists the detachment of droplet during the short-circuiting and thus it is kept of small value.
d) The wire movement gets reversed and the process starts all over again.

1.2 Welding Parameters

I. **Current –** It is one of the most important parameters which controls the welding procedure to a great extent. Along with the weld bead macrostructure, it also influences the penetration. Many trails and literature have shown that an increase in the current value increases the width of the weld bead as well as the depth of penetration. Whereas a decrease in current may reduce the penetration depth and also the weld width becomes narrow [Little (1994)].

II. **Voltage** – A constant voltage arc is generally maintained in this welding technique. The required voltage is set by the operator and the machine then maintains the voltage throughout the welding process [Little (1994)].

III. **Welding Speed** – It is the speed with which the welding nozzle travels over the plates. It controls the metal transfer mode and the penetration in the weld bead.

IV. **Wire feed Rate** – It is the rate with which the feed wire travels through the nozzle towards the weld bead. It controls the shape of the bead as well as the metal deposition in the weld bead [Little (1994)].

V. **Shielding Gas Flow Rate**- It is the rate by which the shielding gas flows. A shielding gas protects the welding arc from the surrounding impurities and thus helps to get a defect-free weld. A stable flow rate is desirable for processes as a lower flow rate results in insufficient shielding whereas a higher rate of flow interferes with the arc stability [Zhang et.al (2013)].

VI. **Arc length correction factor**- Arc length is the distance between the end of the filler wire and workpiece material. An arc length correction factor is also an important parameter to determine the tensile strength apart from heat input and welding speed. A

positive arc length provides better strength and complete penetration [Kannan et.al. (2019)].

VII. **Contact tip to work-piece distant (CTWD**) – It is the distance between the contact tip of the filler wire and the work-piece surface. As we increase the CTWD, the welding current decreases and so is the penetration.

1.3 Stainless Steels

Stainless steels are the iron alloys with a chromium content of more than 10.5% which prevents it from corrosion and imparts heat resistant properties in them. Stainless steels are of many types and each type is classified into several different grades. Each stainless steel grade differs from each other in some property or composition. Other than chromium, some of the other elements present in stainless steel are Carbon (C), Nitrogen (N), Aluminium (Al), Silicon (Si), Sulphur (S), Titanium (Ti), Nickel (Ni), Copper (Cu), Selenium (Se), Niobium (Nb), and Molybdenum (Mo).

Stainless steels because of their exceptional properties like corrosion resistance, workability without much maintenance, and physical qualities are the most preferred and an ideal material for many applications that require strength along with durability without any rusting or corrosion. The size of stainless steels can be altered accordingly and hence it is available in several forms and shapes such as sheets, plates, bars, wires, and tubing. Stainless steels have a wide area of applications and some of the places where It is most commonly used are kitchen appliances, surgical equipment, constructions, and other major appliances and in almost all the industries like paper, chemical, water treatment, and other related factories.

Some of the major advantageous properties of Stainless Steels are:

1. Corrosion-resistant
2. High toughness
3. A High rate of work hardening
4. High hot strength
5. Highly ductile

6. High hardness and strength
7. Low maintenance

1.3.1 Types Of Stainless Steels:-

1) **Ferritic** – They are a type of stainless steel having chromium and small carbon content (< 0.1%). The microstructure of these steels is similar to that of low alloy steel. They usually lack toughness and thus their use is restricted to thin sections. They are mostly used in applications where welding is not required. Hardening them by heat treatment is complicated. They have resistance to stress corrosion cracking (SCC) and are magnetic in nature.
2) **Austenitic** – Most commonly used stainless steel type whose microstructure is composed of Nickel, Manganese, and Nitrogen elements. Austenitic steels have structures similar to ordinary steels at higher temperatures thus improving their characteristic of weldability as well as formability. Standard steel of this type is vulnerable to SCC but it can be reduced by adding Nickel into them. They are non-magnetic in nature but may possess some magnetic response after it is work hardened.
3) **Martensitic** – They are very much similar to ferritic stainless steels based on chromium content but have higher carbon content than that (equal to 1%). These steels are used in the application which requires higher strengths and medium corrosion resistant property. They are mostly preferred in long product application over sheet and plate form. The weldability and formability are lower in them. Also, they are magnetic in nature.
4) **Duplex** – This type of steel has a microstructure comprised of 50% austenitic and 50% ferritic steels. Thus their strength becomes higher than the two. These are SCC resistant. They have a standard resistance to corrosion cracking and other types of corrosion. They are moderately formable and are also weldable subject to the condition that care is taken in regards to heat input and consumables. They are also magnetic.
5) **Precipitation hardening (PH)** – The strength of these steels improves greatly by the addition of Copper, aluminium, and niobium. Proper heat treatment helps in

producing a fine metal matrix which increases the strength. These steels are very much preferred for complex shapes as it experiences very small or no distortion upon final heat treatment. These steels are also resistant to corrosion.

1.4 Austenitic Stainless Steel

Austenitic stainless steels are the biggest member of the stainless steel family and about two-thirds of the total stainless steel produced. They have an austenitic microstructure and a face-centered cubic structure. Elements like nickel, manganese, and nitrogen are alloyed with steel to achieve this microstructure and maintain it in all temperatures extending from cryogenic to the melting point region. Due to this, austenitic steel is not hardenable.

Austenitic stainless steels have lower yield strength in the range of 200-300 MPa and thus they are not much preferred in load-bearing and structural applications. They have high ductility and so are elongated easily. Austenitic stainless steel is mostly used in the form of thin sheets and bars. They can easily be strengthened by the cold working process.

Austenitic stainless steels are further categorized into two sub-groups:-

- **200 Series**- They are Nickel- chromium -manganese alloys, which maximizes the utilization of nitrogen and manganese to minimize the nickel. Because of the introduction of nitrogen in them, they experience an increase in their yield strength by approximately 50% than 300 series.
  Some of the examples of stainless steels of this grade are SS 201, SS 202, SS 205.

- **300 series**- They are chrome-nickel alloys. The introduction of nickel in them helps in achieving the austenitic microstructure. This grade is the largest and the most used stainless steel. In some of the type of steels of this grade, nitrogen is added to reduce the requirements of nickel
  Some of the examples of stainless steels of this grade are SS 301, SS 302, SS 304, SS 308, SS 316.

1.4.1 Properties and Applications of SS 202

Austenitic steel of grade 202 is popular a Chrome-Nickel-Manganese Stainless and is similar in properties to the SUS 302 / A240. It is known for its excellent toughness at a lower temperature. It is widely used for its unique properties like high corrosion resistance, higher toughness, strength, and hardness.

1.4.1.1) Chemical Composition

- Iron (Fe) - 68%
- Chromium (Cr) – 17-19%
- Manganese (Mn) – 7.50-10%
- Nickel (Ni) – 4-6%
- Silicon (Si) - <1%
- Nitrogen (N) - <0.25%
- Carbon (C) - <0.15%
- Phosphorous (P) - <0.06%
- Sulphur (S) - < 0.03%

1.4.1.2) Mechanical Properties

- Tensile Strength – 515 MPa
- Yield Strength – 275 MPa
- Elastic Modulus - 207 MPa
- Poisson's Ratio – 0.27 – 0.30
- Elongation at breaking – 40%

1.4.1.3) Manufacturing Process

Machinability of a SS 202 grade produces long and gummy chips. Machining in them can be performed easily in the annealing condition. The heat treatment process includes soaking the material at about 1038oC for about half an hour (30 mins) and then cooling it below 16 oC to attain full martensitic transformation.

Welding can easily be done in this material by commonly used fusion or resistance methods. Anyhow, it is not advisable to use the Oxyacetylene method for joining. Forging can be performed on this material only after pre-soaking it for at least 1 hour at 1177 oC. Forging at a temperature below 1010 oC must be avoided.

1.4.1.4) Applications

The SS 202 can be easily converted into plates, coils, and sheets as per requirements. Some of the popular applications of this steels are:-

1. Restaurant equipment
2. Kitchen Utensils
3. House Sinks
4. Automobile Trims
5. Architectural Applications
6. Railway Wagons and Cars
7. Trailers
8. Hose clamps

1.4.2 Properties and Applications of SS 304

SS 304 grade is similar to SS 202 in most of the properties. The only difference is the chemical composition as they have high nickel and chromium content. SS 304 is typically furnished into the number of finishes in these following forms such as sheets, strips, tubes, quarto plates, bars, pipes, etc.

1.4.2.1) Chemical Composition

- Carbon (C) – 0.0-0.07%
- Manganese (Mn) – 0.0-1.0%

- Silicon (Si) – 0.0-1.0%
- Phosphorous (P) – 0.0-0.05%
- Sulphur (S) – 0.0-0.02%
- Chromium (Cr) – 17.05-19.5%
- Nickel (Ni) – 8-10.5%
- Nitrogen (N) – 0.0-0.11%
- Iron (Fe) – Balance%

1.4.2.2) Mechanical Properties

- Tensile strength – 540-750 MPa
- Proof stress – 230 MPa
- Elongation – 45%

1.4.2.3) Physical Properties

- Melting Point – 1400 ^{o}C
- Modulus of Elasticity – 193 GPa
- Electrical Resistivity – 0.072 x 10-6 Ωm
- Thermal Conductivity – 16.2 W/m.k
- Thermal Expansion – 17.2 x 10-6 /K
- Density – 8.00 g/cm3

1.4.2.4) Manufacturing Process and Welding

The SS 304 cannot be hardened by a heat treatment procedure. Annealing or a solution treatment is mostly done by a rapid cooling followed by heating to about 1010-1120 ^{o} C. The machinability of SS 304 is of high quality and it Can further be enhanced by following certain rules. The performance of a fusion-welded SS 304 is of excellent quality with or without the use of filler wire. Anyhow, the filler wire electrode

recommended while welding of SS 304 is grade 308. Sometimes heavily welded region requires heat treatment annealing post welding.

1.4.2.5) Application

SS 304 is most widely used in:-

1. Splash and the Sinks back
2. Kitchen Cutleries
3. Saucepans
4. Architecture Panels
5. Tubing
6. Breweries and Dairies
7. Pharmaceutical and food processing equipment
8. Springs, nuts, bolts, and screws

CHAPTER 2: LITERATURE REVIEW

2.1 Introduction

Literature review is scrutinised from previous experimental works and results of various researchers to get a clear picture of the work done in the field of CMT welding and joining of dissimilar metals. [Yan et.al. (2010)] in his study about the physical and metallurgical properties of stainless steels showed in his results the presence of delta ferritic and gamma ferritic phase in its microstructure. [Kumar et.al. (2016)] in his experimentation on the effects of CMT welding process on aluminium found that an increased heat input and better fluidity can be achieved at a lower welding speed. [Varghese et.al. (2019)] in his experimentation of coating inconel 617 M on austenitic stainless steel by CMT welding process found a direct relation between the heat input per unit length and the welding current. Similarly, [Sathiya et.al. (2005)] in his study about the properties of stainless steel of grade 304 with friction welding and concluded on the basis of fractography that fissure occurred most of the times at the joint zone rather than base metal. On investigating tensile specimens, he found an inverse relation between friction time and joint strength. [Sammaiah et.al. (2010)] in his study on metallurgical properties of friction welded aluminium and austenitic steels showed an increase in the tensile strength with decrease in the toughness with an increase in the pressure due to friction.

[Mishra et.al. (2014)] in his investigations about the strength of mild steel welded with different grades of steel found that the welded joints of SS 202 and mild steel gave the best tensile strength value with TIG and MIG welding as well. the welding of dissimilar grades of SS304 and SS202 is meaningful as it will help in future studies. Both SS304 and SS202 are austenitic grade steels containing gamma iron under equilibrium cooling condition. But during rapid cooling, an incomplete transformation occurs which leads to formation of some meta-stable comprising delta iron [Decroix et.al. (1968) and Hanninen et.al. (2001)]. In a study, while investigating the physical properties of inoconel 718 welded with SS316, it was concluded that dissimilar weld gave a higher tensile strength than the parent SS316 metal [Ramkumar et.al. (2017)]. Investigations and analysis have shown that most of the failures occurred in the heat affected zone (HAZ) [Joseph et.al. (2005)]. Studies have proved that SS308 is the most suitable filler wire material for joining SS304, SS321 and SS347. Also this filler wire is most suitable for lower

temperature applications [Dupont et.al. (2007)]. Further experimental results have revealed that arc length correction while joining must be non-linear. Also this results in a controlled dilution in the weld zone which has an advantage during joining of sheets [Cai et.al. (2017)]. Most of the investigations on the welding are carried on the sheets or plates of similar equal thickness. Though, most of the welding required between the automotive parts are between materials of dissimilar thickness [Williams et.al. (2005) and Zhang et.al. (2005)].

In the present research, the mechanical characteristics such as hardness, tensile strength, and residual stresses in the CMT welded dissimilar stainless steel of different thickness plates were found. The residual stresses are the internal stresses that remain in the bodies when subjected to uneven or non-uniform temperature conditions when no external load is applied [Okumura et.al. (1982), Withers et.al. (2001),Wan et.al. (2007) and Vieira et.al. (2013)]. The residual stress measurement is an important issue for understanding the mechanical behavior of materials. If we know the distribution and location of the residual stresses and types of stress in material then the tensile and fatigue properties in the specimens can be predicted easily [Mishra et.al. (2014) and Gupta et.al. (2019)]. The X-ray diffraction method for measuring these stresses are widely used for analyzing the mechanical structures whose static behavior can be studied from a microscopic as well as macroscopic range [Withers et.al. (2008)]. A three-dimensional residual stress was evaluated by [Sasaki et.al. (2013)] obtained by the measurement methods of Dolle-Hauk and Sasaki-hirose. Summary of literature review is exhibited as in Table 1.

Table 1. Literature Review

Sl. No	Author	Process	Material And Filler Metal	Process Parameters	Key Results
1	Wenhu Lin et.al. (2018)	Cold Metal Transfer welding	TC4 ($\alpha + \beta$ phase) and SS 304 (2 mm thick plates) ERCuSi-A (AWS A5.7) wire of 1 mm thickness	Shielding Gas- Argon (99.9 %) Gas Flow-25 Ltr/min Welding speed- 45 cm/min Gap between the plates- 0.75 mm Wire Feed - 3.5 m/min – 5.5 m/min Welding Current- 60-100 A Welding Voltage- 10.8- 11.3 V	1) The highest strength obtained was 294 MPa and the facture occurred on the TC4 plate at the interface. 2) The reinforcements, interfacial layer width and the ultimate strength of the joints increases as the speed of the wire feed was increased.
2	Hulya Durmus et.al. (2014)	Cold Metal Transfer Welding	Galvanised 1314 steel and Aluminium alloy AA 1050 2 mm thick AA 1050 filler wire	Sielding Gas- Pure Argon Welding Current- 107-121 A Welding Voltage- 17.5-18.2 V Wire Feed - 4.8-5.8 m/min Welding Speed- 1.5-2 m/min	1) A proper joint without any burn through can be achieved while welding thin plates by CMT welding because of their low heat input feature. 2) This welding technique due to its exceptional features gives high strength and hardness values along with a pores free weld joint. 3) Smaller the joint gap, higher is the quality of the weld bead achieved.
3	Debashis Mishra et.al. (2019)	Gas Metal Arc Welding	SS 310 and SS 304 (3 mm thickness) 316 of 1.2 mm thickness	Sielding Gas- Argon (99.9%) Welding Current- 80 A Welding Voltage- 19 V	1) GMAW provides joints of better strength for dissimilar joints of austenitic stainless steels. 2) The Strength obtained at the weld bead is highest whereas the joint is weak at heat affected zone. 3) Weld zone has the highest value of hardness.
4	Caimei Wang et.al. (2020)	Tungsten Inert Gas welding	Austenitic SS 304 and Ferritic stainless	Gas Flow rate – 11 Ltr/min Welding Current- 80	1) After the welding is done, the rapid cooling leads to transformation of austenite into martensite and so is the

			steel SS430 of thickness 1.5 mm	A Welding speed – 200 mm/s Arc length- 2.5 mm	hardness. 2) The corrosion resistance of the fusion zone increases due to the increment in the chromium content.
5	Gurdeep singh et.al. (2020)	Gas Tungsten arc welding	Austenitic SS 304 and copper 1 mm thick	Sielding Gas flow rate – 12 Ltr/min Current- 90 A Voltage- 11 V Welding Speed- 1.44 mm/s CTWD- 1.6 mm	1) A perfect joint can be achieve while welding dissimilar austenitic materials. 2) Fracture appears to be satisfactory as it initiates with necking. 3) The necking initiates at the heat affected zone and failure occurs in this region only.
6	S.K. Rajput et.al. (2019)	Gas Metal Arc Welding	Austenitic stainless steel SS316 and Ferritic stainless steel SS409 of thickness 6 mm SS 308L of thickness 1.2 mm	Shielding Gas- Pure Argon Gas flow rate – 23 Ltr/min Current- 220 A Voltage- 24 V Welding Speed- 5 m/min	1) Maximum hardness obtained at weld zone because of the addition of filler material. The trend decreases from the weld zone towards the HAZ. 2) Hardness also is dependents on the heat input as lower the heat input higher is the hardness. 3) Coarser grains at the HAZ in the austenitic plates is observed thus this region becomes smooth.
7	H. Vinothkumar et.al. (2020)	Gas Tungsten arc welding	Austenitic Stainless steels SS 303 and SS 316 of Thickness 6 mm	Shielding gas- Argon Gas flow rate – 18 Ltr/min Current-120–150 A Voltage - 16–18 V Travel speed - 3.5 mm/min Stand-off distance – 3 mm	1) The fracture happens in one of the base plates and this shows that the weld zone always is of higher strength. 2) During the welding of austenitic steels, due to rapid cooling the fusion zone converts to delta ferrite thus making it strong and hard.
8	S. P. H. Marashi et.al. (2009)	Resistance Spot Welding	Low carbon steels of thickness 1.25 mm and 2.5 mm	Welding Current- 10 kA Electrode force- 4.2 KN	1) The weld zone of dissimilar thick joint is asymmetrical. 2) In a dissimilar thickness joint, necking initiates followed by failure in

			thick	Holding Time- 30 cycle (1 cycle = 0.02 sec) Welding Time- 9-18 cycles	the thinner base plate.
9	Dewin Purnama et.al. (2019)	Gas Metal Arc Welding	SS 304 and low carbon steel SS 400 of thickness 3 mm Filler wire SS 308 and SS 316 of thickness 1.2 mm	Shielding Gas- 90% Argon + 10% Carbon and Carbon 100 %	1) Selection of filler wire is a factor that determines the microstructure of the fusion zone. 2) Small amount of carbon along with argon is preferred as the shielding gas as it acts as a better protector. It protects the welded joint from the atmospheric gas impurities and also less inclusions are observed in the macroscopic image. 3) SS 308 is resistant to sulphur at high temperature. It has high ductility and toughness. Due to its easiness in fabrication and machinibility, it is highly preferable.
10	A. Ravisankar et.al. (2018)	GTA Welding	Modified steel P91 and SS 304 of thickness 3 mm	Heat Input- 435 J/mm Velocity- 1 mm/s Efficiency- 0.7 Q_f/Q_r – 0.25	1) Residual stress in a body depends upon the eigen strain and the mechanical properties of the material. 2) A martensite formed in the joint results in the presence of compressive stresses. 3) Residual stresses in dissimilar joints are slightly higher than similar welded joints.
11	A.B. Verma et.al. (2014)	Resistance spot welding	Austenitic stainless steels SS 304 and SS 316 of thickness 0.6 mm	Electrode material- Chromium alloy Current- 5-7 kA Time- 5-7 Cycles Pressure- 2-2.5 kg/cm^2	1) Tensile strength of dissimilar welded materials were observed to be higher than the strength of the joint of similar material. 2) Current is the most important parameter that has an impact approx. 66.94% on the strength of dissimilar weld produced.

					3) The hardness value obtained at weld zone is highest while welding dissimilar austenitic materials.
12	Sahil Bharwal et.al. (2014)	Gas tungsten arc Welding	Austenitic SS 304 (thickness 6 mm) and SS 202 (thickness 6 mm)	Shielding gas- Argon Gas flow rate – 6 Ltr/min Current-160 A Welding speed- 2.5 mm/s	1) The strength values obtained states that it is fairly enough to use SS 202 in different applications. Due to reduced nickel content, it is available at lower cost and thus can be used in place of SS304 in most applications. 2) The matrix in the fusion zone converts to delta ferrite from austenite because of rapid cooling.
13	Rahul Kumar Keshari et.al. (2019)	Gas Tungsten arc Welding	Austenitic stainless steels SS304 and SS 202	Comparison of Filler Metal SS 308 and SS 316	1) The join obtained by the filler metal SS 308 is of higher strength due to the refined grain structure and distinctive metal composition. 2) The Micro-Hardness obtained was highest for the welded joint with SS 308 filler wire due to proper fusion. 3) The weld strength or tensile strength of SS 202 depends a lot on the process parameters and use of filler wire. 4) The measure of micro-hardness is a significance of tensile strength of material. The welded joint between SS 304 and SS 202 fails at SS 202 basically due to low hardness.
14	Hongduo Wang et.al. (2019)	Friction Stir Welding	Austenitic SS 304 and Low carbon steel Q235 of thickness 3 mm	Rotational Speed- 475 Rpm Welding Speed- 47.5 mm/min Welding Pressure- 20 kN	1) The micro hardness trend starts to decrease as we move from BM to HAZ and the trend increases as we move towards WZ. The value of micro hardness is maximum at weld zone for the dissimilar material joints. 2) The dissimilar welded joints have higher strength than base metal joints.

15	Rajesh Kannan A et.al. (2019)	Cold Metal Transfer Welding	Austenitic Stainless Steel SS 316 of thickness 2 mm SS 308 of Diameter 1.2 mm as filler wire	Shielding Gas- Argon(98%)+ Carbon-di-oxide (2%) Gas Flow Rate- 20 L/min Current- 105 A Voltage- 12.5 V Welding Speed- 350 mm/min Arc Length Correction- -20% to 20%	1) The top reinforcement of the welded joint increases with an increase in arc length correction factor from a negative value to positive value. 2) The arc length correction factor controls the tensile strength of the welded austenitic steel to some extent. The obtained strength is more for positive arc length correction factor. 3) 10% arc length correction factor produces the best strength and weld bead profile.
16	Eddy Gunawan et.al. (2012)	Gas Tungsten arc welding	SS 400 Plate and SS 304 SS 308 is used as filler electrode	Current- 80 A and 100 A	1) The tensile strength for the maximum current value was highest and it showed that strength increases as the welding current increases.
17	Ali Mehrani Milani et.al. (2016)	Cold Metal Transfer Welding	Aluminum Alloy 5754 (Thickness 3 mm) and Galvanized Steel (Thickness 2 mm) AlSi3Mn of diameter 1.2 mm used as filler wire	Shielding Gas- Argon Gas flow Rate- 17 L/min Welding Speed- 10 mm/s Stick out- 17 mm	1) Pulse correction factor is a parameter that determines the properties of welded joint. 2) The width of the seam and the throat of weld size increases with filler wire flow which increases due to an increase in the pulse correction factor. 3) The tensile strength and width of inter-metallic layer increases with an increase in the pulse correction factor.
18	Gulshan et.al. (2015)	Resistant Spot Welding	Low Carbon steel (Thickness 1.51 mm) and Austenitic Stainless Steel (1.48 mm)	Current – 3-9 kA Voltage- 5 kVA Frequency- 50 Hz Cooling water flow rate- 6 L/min Holding time- 5 cycles Weld Force- 4 KN	1) Weld nuggets formed in a dissimilar welded joint are of asymmetrical shape. 2) The size of nugget increases with an increase in the current value. 3) Strength of joint with maximum current is highest. 4) The hardness value obtained is maximum at weld zone.

19	Raghuram et.al. (2019)	Tungsten Inert Gas (TIG) Welding and Metal Inert Gas (MIG) Welding	SS 202 and SS 304 of thickness 6 mm		1) SS 308 is most suitable filler wire for welding Austenitic stainless steel of grade 304. 2) The base metal of both the materials of the welded joint has an austenitic microstructure whereas the grain size becomes coarser in the heat affected zone. 3) The properties of welded joint depends a lot on the welding parameters chosen.
20	Triyono et.al. (2011)	Resistance spot welding	Austenitic Stainless steel 304 of thickness 3mm and 1mm	Welding Current- 4.7 kA Welding Time- 20 Cycles Electrode force- 6 kN	1) The unequal thickness leads to uneven distribution of heat balance, thus more thermal heat generated on thick plate leading to almost 100% penetration in the thicker plate. 2) The hardness of the joint is not much affected by the dissimilar thickness of the joining plates. 3) The crack initiates from the thinner section and propagates until fracture occurs. Most of the fracture occurs at HAZ of thin section. 4) The fatigue strength and the endurance limit of the dissimilar thickness joint was higher. Also the fracture observed was of ductile and brittle nature i.e it initiates with a necking.
21	Bhushan Y Dharmik et.al. (2020)	Cold metal transfer Welding	Cold Rolled Noon-oriented (CRNGO) Electrical Steel (Grade M-45) of thickness 0.5 mm		1) On investigation it was found that lesser losses occurred in the welded joint by CMT than MIG or GTAW. 2) The CMT welding because of its short-circuiting produces lesser accumulation of heat on the material thus lesser coarse grains. 3) CMT welding due to its features is

					most suitable for welding thin sheets.
22	Madhavan et.al. (2017)	Cold Metal transfer welding	Aluminum Alloy A6061-T6 (2 mm) and AZ31B Magnesium alloy (3 mm) Filler wire Al-5 %Si (1.2 mm)	Shielding gas- Pure Argon Gas Flow Rate- 18 L/min Current- 70-100 A Voltage- 12.2-12.9 V Welding Speed- 3.916- 5.083 mm/s	1) Higher heat inputs results in higher tensile strength value and high welding speed leads to minimal heat affected zone. 2) The fusion zone is directly proportional to heat input thus fusion zone width increases as the heat input increases and the fusion zone has a direct impact on the joint strength.
23	Zhang et.al. (2009)	Cold Metal Transfer Welding	Aluminum 1060 (Thickness 1 mm) and Zn-coated steel (Thickness 0.6 mm) Al-Si alloy wire of thickness 1.20 mm	Shielding Gas- Argon (100%) Gas Flow Rate- 15 dm^3/min	1) It is possible to weld dissimilar materials of Aluminium alloy and steel sheet without having any cracks CMT technique. 2) The Inter-metallic Layer (IML) which has its thickness under 5 μm, consists of Fe_2Al_5 and $FeAl_3$ phase between steel and weld metal interface.
24	D. Delbergue et.al. (2016)	X-Ray Diffraction Technique	Martensitic Steel of thickness 0.798 mm	Proto iXRD diffractometer- $\sin^2\psi$ method Pulstec μ-X360 apparatus - cos α method X-Ray Tube Voltage – 30 kV	1) Stresses computed by X-Ray diffraction are linearly connected to the Elastic constants of X-Ray. 2) The measurement by Cos α method which is a 2D detector technique gives better result than $\sin^2\psi$ method. Also this device is simpler and lighter than the one using the latter technique.

2.2 Heat Input Calculation

The properties of the weldment produced depends on the heat input to a great extent and it also controls the rate of cooling which has an impact on the microstructure formed [Irizalp et.al. (2016)]. The heat input can be easily calculated from equation 1 as shown below [Cook et.al. (1985)]. A process is said to be efficient if it produces a stronger joint with a lesser heat input [Mandez et.al. (2001)].

$$Q = \eta \frac{V.I.60}{S.1000} \quad \ldots\ldots\ldots\ldots\ldots\ldots\ldots\ldots\ldots\ldots\ldots\ldots(1)$$

Where Q is the heat input (KJ/mm)

V is the voltage (V)

I is the current (A)

S is the welding speed (mm/min)

2.3 Summary of Literature Review

The various processes of welding, their process parameters and welding material combinations along with the mechanical and micro-structural study of the welded joints stated by various researchers are discussed. The interferences drawn from the prominent results of Table 1. are :-

1. In CMT, the retractive movement of the filler wire during the course of short circuit plays an important role by diminishing the formation of spatter thus eliminating any post-weld machining requirement and produce weld of high quality.
2. The optimum process parameters depends on a number of factors mainly the type of material chosen, the filler wire metal, the arc correction factor and other surrounding conditions.
3. The heat input as well as the penetration in the fusion zone are greatly influenced by the wire feed rate and the welding speed. With an increase in the wire feed rate and a lesser welding speed, a increased heat input is achieved along with a weld bead with higher penetration.
4. The joint strength of dissimilar austenitic stainless steel welds are higher due to incomplete transformation of austenite into delta-ferrite microstructure in the fusion zone because of the rapid cooling.
5. The fatigue strength and the endurance limit of joints of dissimilar thickness is higher than that of joints of base metals of similar thickness anyhow dissimilar thickness leads to uneven heat distribution. The hardness value is unaffected by the dissimilar thickness.

2.4 Research Gaps

1. The research in the area of joining thin stainless steel sheets is very limited and it needs to be explored.
2. The field of joining dissimilar austenitic steels of grades 202 and 304 of different thickness by CMT welding technique has yet not been explored by the researchers.
3. Although many different types of work-piece materials, filler wires, arc length correction factor of different levels has already been considered by many authors but all these parameters together for welding austenitic steels of grades 202 and 304 are not yet studied.
4. It is evident from the literature review that the industrial application based research of stainless steels of grade 202 and 304 are yet to be implemented.

CHAPTER 3: EXPERIMENTAL PROCEDURE

3.1 Material And Methods

In the present experimental work, welding of SS 202 and SS 304 of dissimilar thickness of 1.2 mm and 2 mm respectively was done by CMT welding technique as shown in Fig. 3. using SS 308 of thickness 1.2 mm as filler material for welding wire. Recent advancements in modern industry have found a number of applications of tailor welded blanks (TWB) which are made from single sheets of steel of dissimilar thickness, coating and strength which are welded together. Flexible part designs are allowed in this manufacturing procedure and it is ensured that right amount of material is used at the right place. The shielding gas in this experiment is a mixture of 98% argon and 2% carbon. During the process of welding, the shielding gas usually interacts with the filler metal which results in microstructure advancements thus influencing the mechanical as well as corrosion resistance properties of the weld deposits. An increase in CO2 % in the Argon + CO2 mixture leads to increased spatter rates and decrease in the ferrite numbers. It also improves the wettability of molten filler wire and fusion volume. SS 202 and SS 304 plates selected for the experimentation were cut in the size of 100 mm × 50 mm x 1.2 mm and 100 mm x50 mm x 2 mm respectively. The weight percentage composition of SS202 sheet and SS 304 sheet is given in Table 2. and Table 3. respectively.

Fig. 3. CMT Welding Machine

Table 2. Chemical Composition of SS 202

Fe	C	Si	Mn	P	S	Cr	Mo	Ni	Al
73.9	0.103	0.490	10.5	0.0730	0.0179	12.8	0.303	0.205	<0.002

Table 3. Chemical Composition of SS 304

Fe	C	Si	Mn	P	S	Cr	Mo	Ni	N
71.9	0.0585	0.219	0.837	0.0426	0.0166	18.3	0.157	8.28	0.1

3.2 Taguchi Optimization Technique

To get a quality weld bead aesthetics, it is very important to carry out a number of trial experiments. The Design of Experiments (DOE) is basically a technique by which a set of parameters are selected based on trials and reviews and experiments are performed using these parameters to obtain a set of optimized parameters along with their relationship [Shanmugasundar et.al. (2019)]. While performing these set of designed experiments, any changes made in the input parameters are reflected in the form of changes in the output parameters. Taguchi L9 method is an optimization technique that optimizes the total number of experiments to be performed to draw a conclusion when many variables are present. In Taguchi method, the optimization using different parameters are carried out by identifying and evaluating the input variables and their interactions. And then the input variables are assigned to the orthogonal array arrangements to perform the experiments. The parameters for the welding process and their three levels are as shown in the Table 4. This design technique determines the influence of input variables on the output response values such as tensile strength, elongation, hardness etc. A main effect plot and S/N main effect plots are generated that show the effect of each individual parameter on the output response and also the best optimal parameter suitable to generate the best output.

Table 4. Working range of Process Parameters

Factors	Process Parameters	Units	Levels		
			1	2	3
A	Welding Current	(Amps)	75	95	115
B	Welding Speed	(mm/s)	4	5	6
C	Arc Length Correction Factor	(%)	-10	0	+10

3.3 Welding Parameters

A number of preliminary trials and tests were done to get current, welding speed and arc length correction factor as the optimum parameters. The parameters are chosen in a way that the plates are welded correctly without any damage or burn through. The thickness ratio of the two plates are 1.67, which may result in local stress concentration and shift in neutral axis and thus clamping is done with utmost care to avoid distortion. Taguchi L9 Optimization technique has been applied here to obtain a combination of optimal parameters mainly the design of experiments for the process.

Here, 3 different levels each for welding current, welding speed and arc length correction factor are utilized to produce 9 different welded specimens on the basis of obtained design of experiments (DOE) by L9 Taguchi's orthogonal array method using the MINITAB 19 software. Table 5. shows the process parameter used during the CMT process having current, welding speed and Arc length correction factor of 3 different levels while keeping the flow rate of shielding gas and contact tip to work piece distance (CTWD) as constant for all the samples respectively. Fig. 4. shows a welded sample with all the parameters on it.

Table 5. Welding Process Parameters

Sample No.	I (A)	W.S (mm/s)	A.C.F (%)	CTWD (mm)
C1	75	4	-10	10
C2	75	5	0	10
C3	75	6	10	10
C4	95	4	0	10
C5	95	5	10	10
C6	95	6	-10	10
C7	115	4	10	10
C8	115	5	-10	10
C9	115	6	0	10
I = Current, W.S = Welding Speed, A.C.F = Arc Correction Factor, Flow Rate Of Shielding Gas = 15 Ltr/Min				

Fig. 4. Welded Samples with different Process Parameters

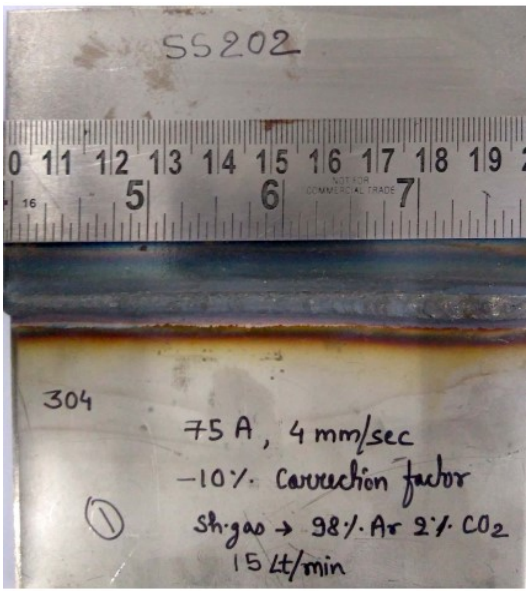

(C1)

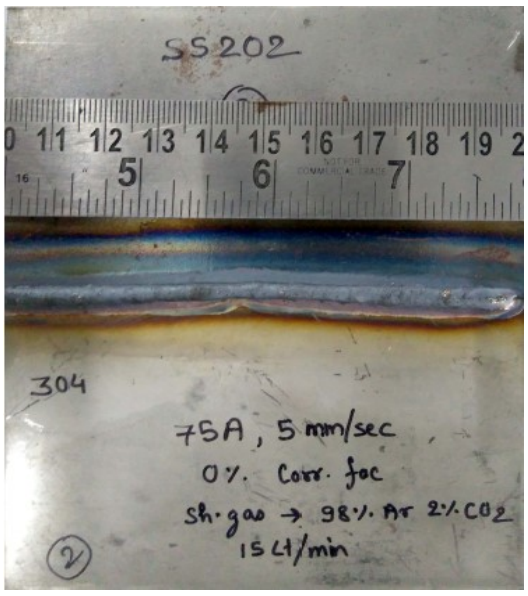

(C2)

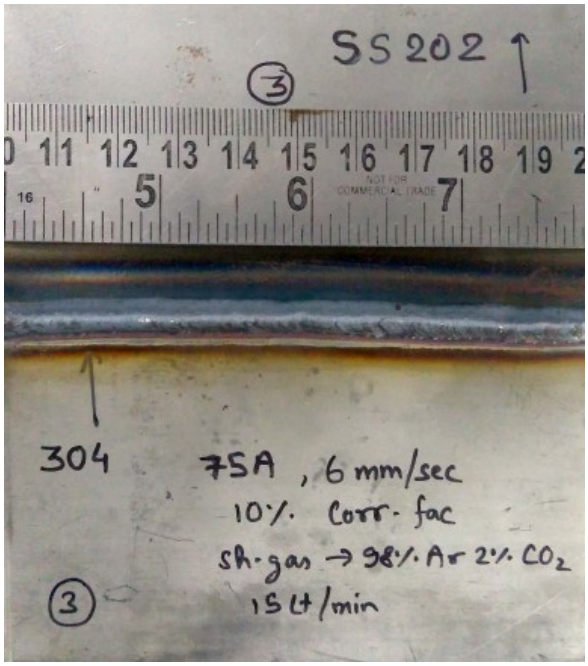
SS 202
3
304
75A , 6 mm/sec
10% Corr. fac
sh. gas → 98% Ar 2% CO2
15 Lt/min
3

(C3)

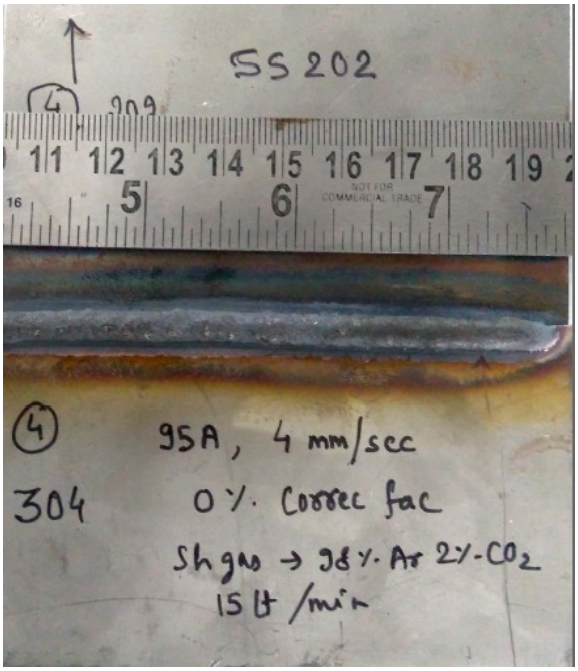
SS 202
4
304
95A , 4 mm/sec
0% Correc fac
Sh gas → 98% Ar 2% CO2
15 Lt/min

(C4)

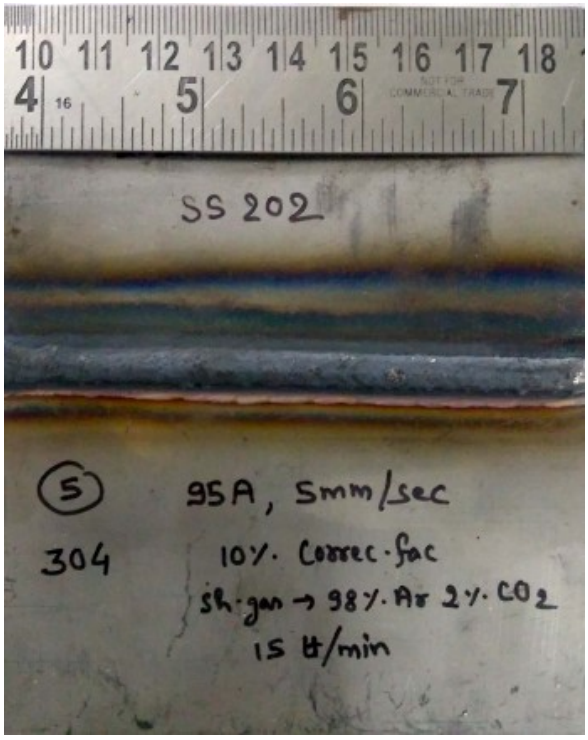
SS 202
5
304
95A , 5mm/sec
10% Correc. fac
sh. gas → 98% Ar 2% CO2
15 Lt/min

(C5)

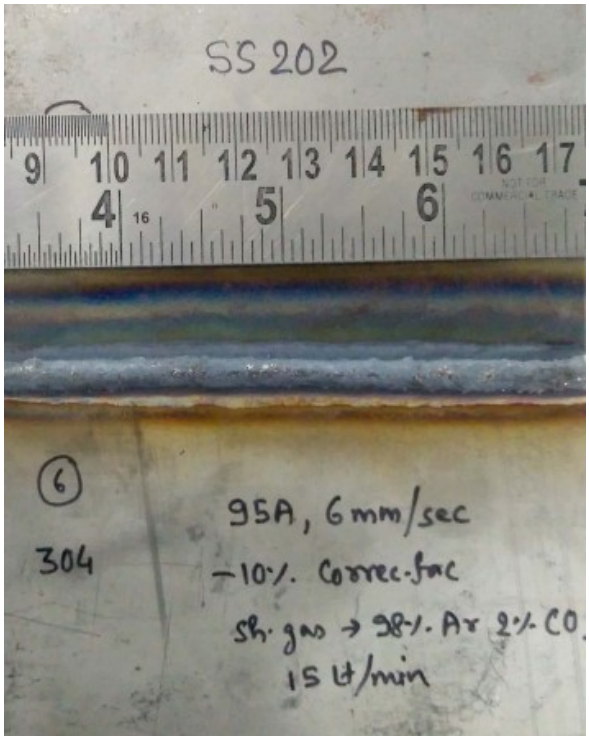
SS 202
6
304
95A, 6mm/sec
-10% Correc. fac
sh. gas → 98% Ar 2% CO
15 Lt/min

(C6)

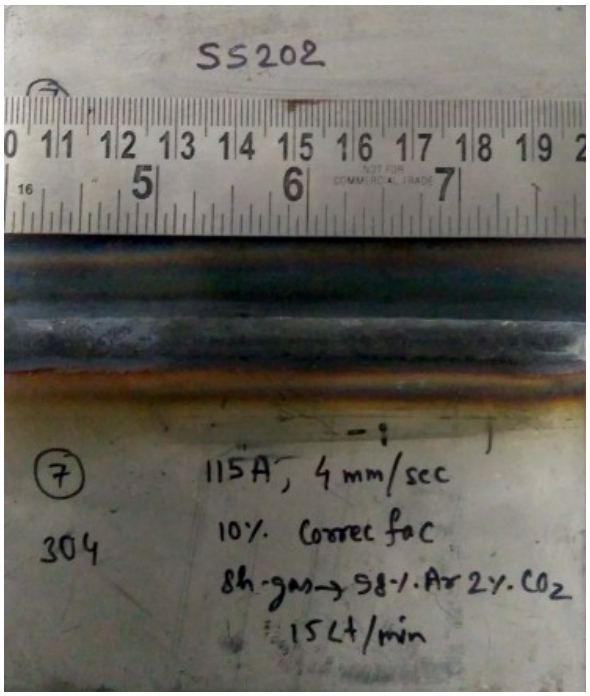
SS202
7
115A, 4 mm/sec
10% Correc fac
304
Sh-gas → 98% Ar 2% CO2
15 Lt/min

(C7)

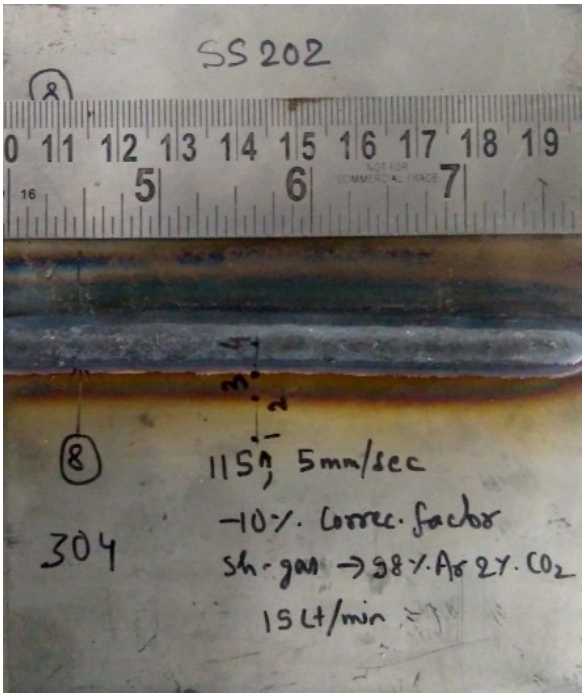
SS 202
8
115A, 5mm/sec
-10% Correc. factor
304
Sh-gas → 98% Ar 2% CO2
15 Lt/min

(C8)

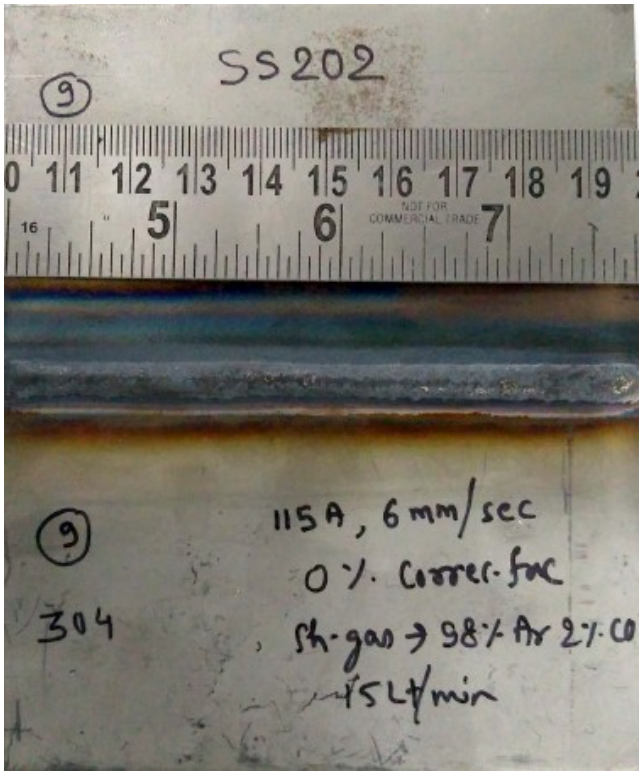
SS202
9
115A, 6 mm/sec
0% Correc. fac
304
Sh-gas → 98% Ar 2% CO
15 Lt/min

(C9)

CHAPTER 4: TESTING METHODS

4.1 Tensile Strength Testing

The usage of any material in an engineering application depends on its mechanical properties like tensile strength, elongation etc. These properties can be determined by tensile testing. Documentation of any new joint formed is necessary as it stabilizes this new joint combination against the already available in the market. The tensile strength of the material can only be quantified by the performance of testing on the material. Tensile testing of a material is done by subjecting the material on Universal Testing Machine (UTM).

The specimen for the tensile testing as per ASTM standards as shown in Fig. 5. were cut using the wire EDM process. Fig. 6. shows the welded plates from which the specimen were cut as per standards. The tensile specimen was of sub-size 100 mm, gauge length 32 mm and gauge width of 6 mm.

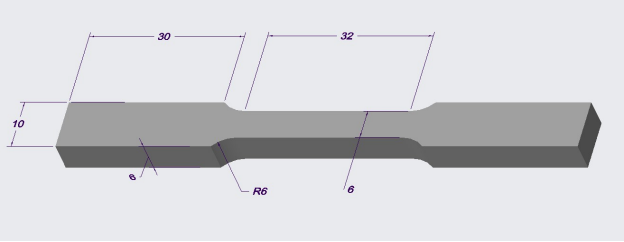

Fig. 5. Tensile testing specimen as per ASTM E8 std.

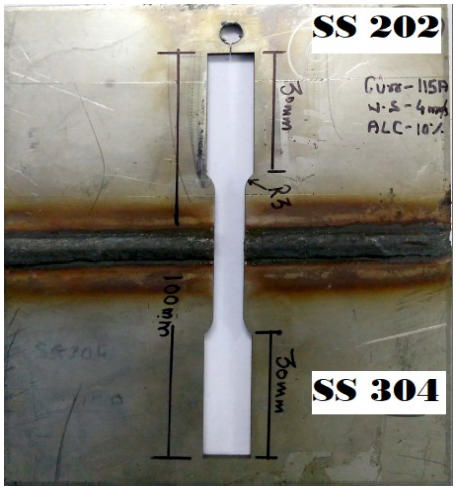

Fig. 6. Welded Joint from which the tensile specimen is cut using EDM

The specimens were tested at all the different parameters to find their strength. Tinius Olsen Ultimate Testing Machine H50KS of 50 KN capacity as shown in Fig. 7. was used to determine the mechanical strength at a strain rate of 1 mm per min at room temperature. The standard tensile properties such as yield stress and ultimate tensile stress were determined.

Fig. 7. TINIUS OLSEN ULTIMATE TESTING MACHINE H50KS

4.2 Micro-Hardness Testing

Micro-hardness testing is basically done to determine the hardness of the joint surface which is actually the measure of the resistance to indentation or penetration on the surface. Microhardness in a welded joint are tested over a small test sample or small region to determine the hardness of the welded surface. The Microhardness testing involves a Vickers diamond indenter which is pressed into the surface of the welded portion with the help of a penetrator and a small load. The load when applied on the surface, it indents causing a permanent deformation on the surface making an impression of the shape of indenter. The pressure applied is monitored and the test is performed under controlled condition within a time segment and a square shape as of the indenter is generated on the surface. The diagonal is measured and using the formulae the Vickers hardness value is calculated. The Microhardness test is done on an instrumented indentation tester as shown in Fig. 8.

Fig. 8. Micro-Hardness Tester

A piece of 10mm x 10mm was cut through the welded section and its cross sectional view was examined for micro-hardness. It was dry polished with emery paper of different grades of sizes namely 120, 180, 240, 360, 400, 600, 800, 1000, 1200, 1500, 1800 and 2500. Specimens were grinded properly for approximately 2-3 mins with each grade. Wet polish is then done where a continuous supply of water is provided in order to reduce friction and make the surface scratch free. Further polishing is proceeded with a velvet cloth using alumina powder. The use of alumina powder is done to obtain a shining mirror like surface. The Fig. 9. shows a surface whose microhardness was found on the microhardness tester.

Fig. 9. Micro-Hardness Specimen

4.3 Residual Stress Measurement

The residual stress which are basically the internal stresses which occur due to non uniform distribution of temperature was calculated using a μ-X360s X-ray residual stress analyzer as shown in Fig. 10. This system consisted of a sensor unit attached to a computer for output result and a power system. The sensor unit uses cos alpha method to calculate the residual stress.

Fig. 10. μ-X360s X-ray residual stress analyzer

As there are many non-destructive techniques for measuring the residual stresses, but X-ray diffraction is suitable for thin plates as its penetration is about 10μm with spatial resolution in the range of 10μm to 1mm Some positions were marked comprising of the base plate (BM), heat affected zone (HAZ) and the weld zone (WZ) on both plates. Also some positions were marked along the weld bead. Full debye-scherrer ring at each position was acquired through X-ray exposure. These rings determined the strain and finally the residual stress value at each position was produced. Residual stress was calculated at five positions for all the samples as in Fig. 11.

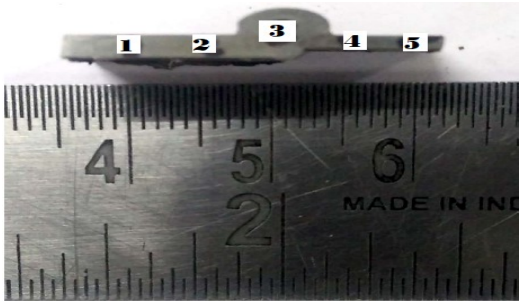

Fig. 11. Sample for Residual Testing

CHAPTER 5: RESULT AND DISCUSSIONS

5.1 Tensile Strength

The testing of each sample at different parameters helped in evaluating the best joint. Fig. 12. shows the specimens for the tensile testing as obtained after EDM cutting and Fig. 13. shows the breaking point of the specimen after the ultimate tensile strength is evaluated.

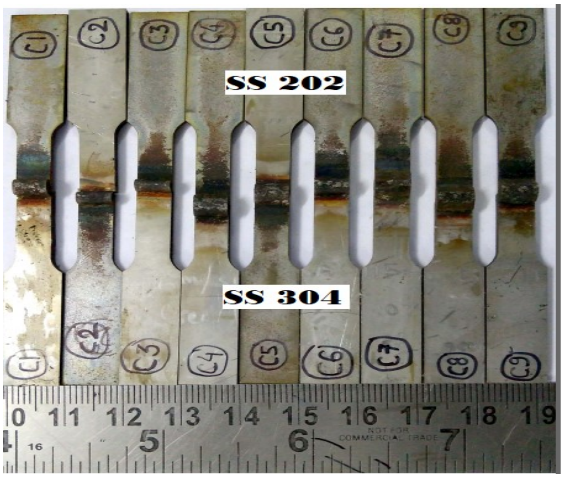

Fig. 12. Tensile Specimens

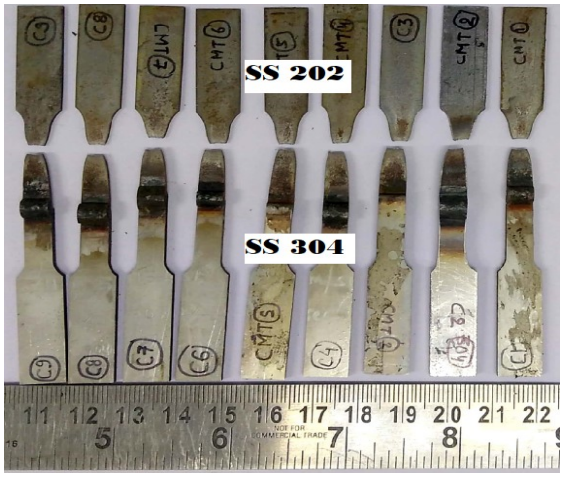

Fig. 13. Specimens post Tensile Test

Welding entails the melting and solidification of the base metal. Welding of dissimilar materials involves fusion of two different materials having different solidification rate. This ultimately changes the microstructure and the grain size. The weld zone bead has high strength due to the alloy genesis. The filler wire along with the melted base metal forms this alloy thus making it the strongest portion. The typical tensile stress-strain graph of welded samples (C1, C4, C5, C7, C8) is shown in Fig. 14. The tensile strength and elongation response results obtained for the welded sample are shown in the L9 orthogonal array as given Table 6. The maximum tensile strength achieved is 291 MPa at 115 A current, 4 mm/s welding speed, and 10 % arc length correction factor. The tensile results show an increase in weld strength as the welding current is increased and no significant change in the elongation was observed. [Prakash et.al. (2017)] reported that sample SS202-SS316 of 1.5 mm sheets spot welded specimen tensile strength was 268 MPa. In this study, the maximum tensile strength value of 291 MPa was achieved. This strength was achieved at 4 mm/s welding speed and 10 % arc length correction factor. Arc length is the

distance between the end of the filler wire and workpiece material. An arc length correction factor is also an important process parameter to determine and maximize the tensile strength of welded material. A positive arc length provides better strength and perfect penetration. [Kannan et.al. (2019)] results support for a significant increase in strength for samples C1, C5 and, C7 with positive arc length correction factor. It was observed that the maximum elongation observed with a higher positive arc length correction factor welded sample.

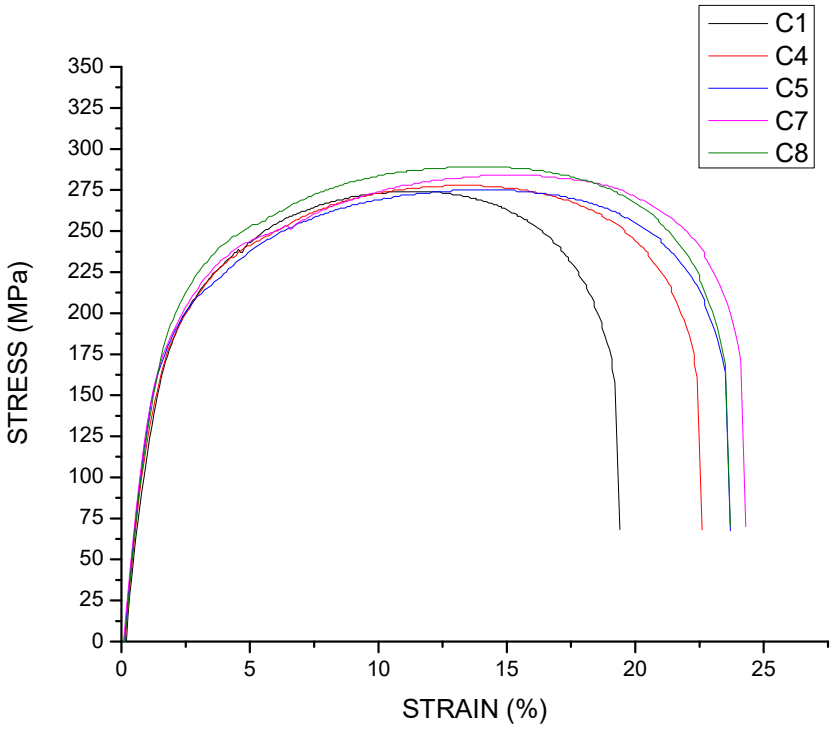

Fig. 14. Typical Stress vs Strain graph of Welded specimen

Table 6. L9 Orthogonal array with Response Variables

SAMPLE NO.	I (A)	W.S (mm/s)	A.C.F (%)	TENSILE STRENGTH (MPa)	ELONGATION (%)
C1	75	4	-10	274	19.2
C2	75	5	0	270	18.3

C3	75	6	10	272	20.4
C4	95	4	0	277	22.9
C5	95	5	10	284	23.1
C6	95	6	-10	275	21.3
C7	115	4	10	291	23.4
C8	115	5	-10	283	22.7
C9	115	6	0	279	21.9

Main effect plots were generated based on the response variables. The main effect plots describes the significance of input variables on the variation of individual output responses. The main effect plots were drawn in a way that the input parameters at different levels were represented on x-axis while the mean average of the responses were represented on the y-axis. The Fig. 15. shows the mean effect plot as obtained by the software. It clearly shows an increase in the trends or values for which the best quality response was obtained. The maximum strength and hardness increases with an increase in the current value and a decrease in the welding speed. A positive arc length correction factor produces a weld bead of high quality.

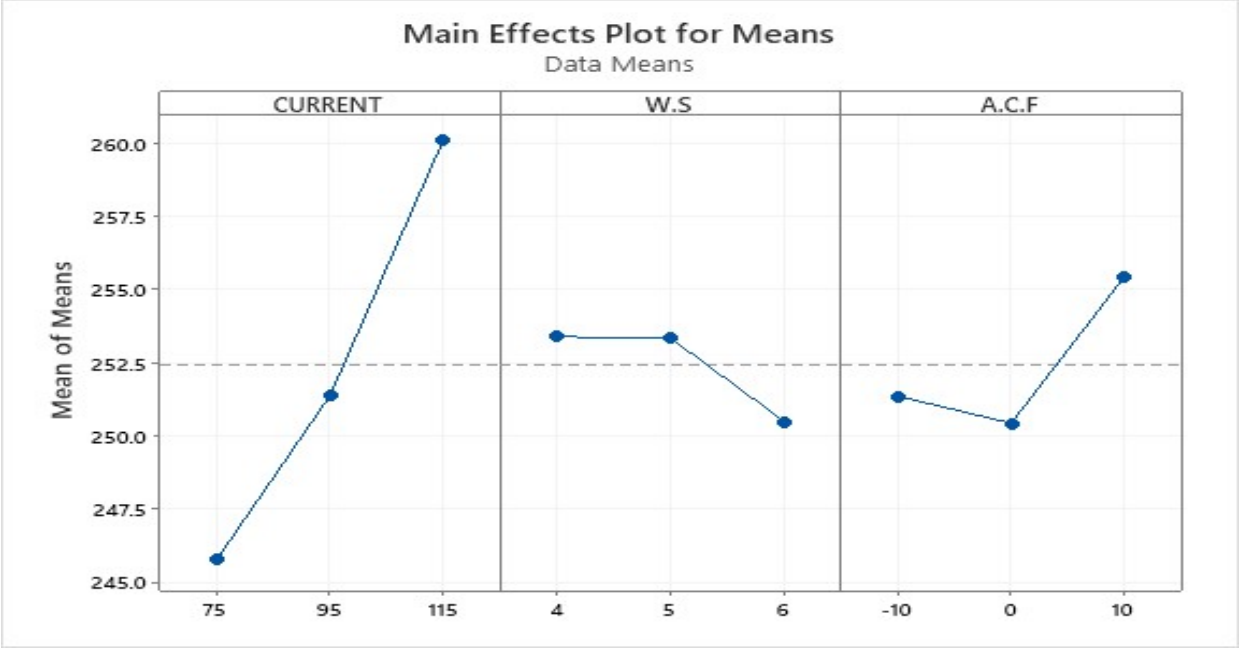

Fig. 15. Main Effects Plots for Response Variables

A S/N ratio main effect plot is also produced which gives the optimal parameters for obtaining the best result. S/N ratio is the method which measures the ability of a characteristics to affect the external factors or uncontrolled noise factors. The Fig. 16. represents the effect of S/N plot for the responses. Results obtained from the plot shows the best quality weld is produced at 115 A current, 4 mm/s weld speed and 10 % arc length correction factor.

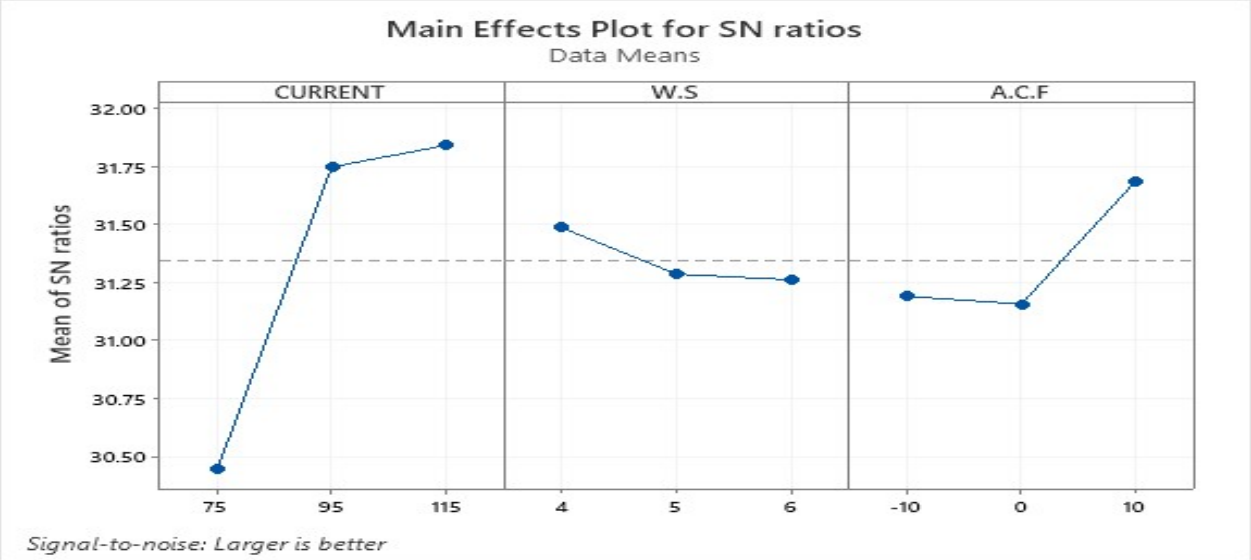

Fig. 16. S/N Plot for the Optimal Parameter

The tensile fracture of the welded specimen clearly shows the formation of a cup-cone shape when necking initiates or due to surface slip occurs. Joining dissimilar material thickness leads to uneven heat distribution and a higher amount of heating takes place in thicker sheets in comparison with smaller thickness sheets. These results lead to maximum penetration in the thicker plate and less take place in thin sheets. [Hasanbasgolu et.al. (2007)] and [Marashi et.al. (2008)] observed that in spot welding of dissimilar thickness material's necking initiated in lower thickness sheets. The thinner sheets occur severe necking due to lesser force. The finite element results have shown the concentration of stress in the thinner section due to plastic distortion in the thinner part [Darwish et.al. (2004)]. The efficiency of the welded joint was 100 % as all the failures occurred in the heat-affected zones (HAZ) of the thinner section of the SS 202 material. These results revealed that evidence of low heat input characteristics of CMT welding provides higher strength joints for dissimilar thickness.

5.2 Micro-Hardness (HV)

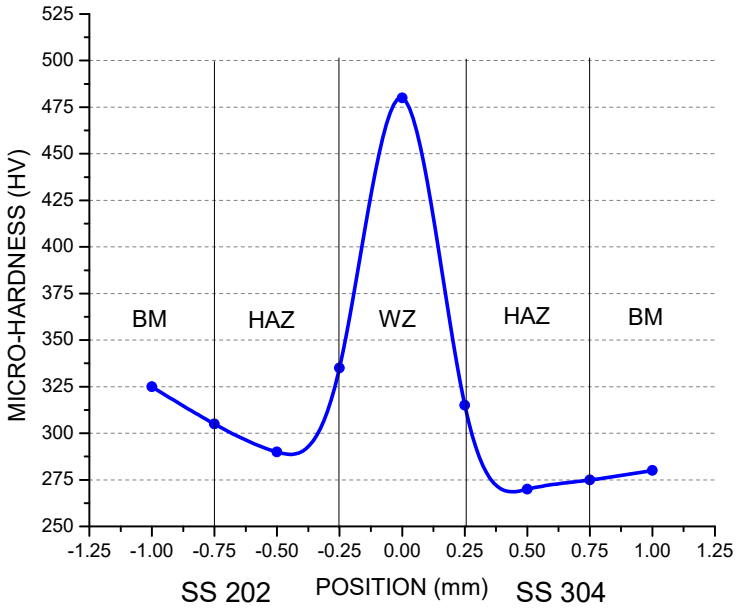

Fig. 17. Micro-Hardness variation for Sample C7 welded at 115 A current, 4 mm/s welding speed, 10% arc length correction factor

Fig. 17. shows the micro-hardness variations for the welded sample C7 welded at 115 A current, 4 mm/s welding speed, and 10 % arc length correction factor with respect to the positions. The higher hardness value was observed on the welded region and decreasing trend in the base metal (BM) and heat-affected zone (HAZ) for both the steel sheets. The micro-hardness of base material SS 202 and SS 304 are 325 HV and 280 HV respectively. The hardness in the material depends upon the carbon content and it controls the presence of cementite. The carbon content in SS 202 is slightly higher than SS 304 thus a difference in the hardness value of the base metal is observed. The micro- hardness of both SS 202 and SS 304 in the heat-affected zone (HAZ) reduces to 290 HV and 270 HV respectively. [Sabooni et. al (2015)] reported that Friction stir welding of SS 304 softening of HAZ takes place due to the recovery of coarser grains. According to the hall-petch relationship, the hardness and strength of a material are correlated to grain size. The reduction of micro-hardness in HAZ due to coarser grains. The hardness of the material relates to tensile properties in a material. The low hardness in HAZ is an important factor for the initiation of crack and fracture took place in this region during the tensile testing.

Hardness is increasing towards the weld region. The increasing trend between HAZ and WZ is due to enhanced refinement grains of the austenitic steels. Similar type of pattern reported in the welding of SS 202 and SS 304 by TIG welding [Keshari et.al. (2019)]. The hardness value achieved by CMT welding is higher than TIG welding. The hardness value of material depends upon the heat input that occurs during welding. Lesser heat input results in harder increases in weld region. The diffusion of chromium element between the two stainless steel sheets increases the hardness of weld zone. The highest micro-hardness value at the weld zone was 480 HV achieved for the C7 sample which is welded at the highest current value (115 A), slow welding speed (4 mm/s) and a positive arc length correction factor (10 %). The micro-hardness value in the welded region in the range of 460-480 HV due to its finer grain structure and excellent fusion of filler wire in the weld zone. Besides that the high rate of cooling in CMT process and an incomplete austenitic transformation in weld zone forms delta-ferrite phase. These are reasons for increasing the hardness in the welded region. Fig. 18. shows similar types of results for samples C1, C4, C5, and C8.

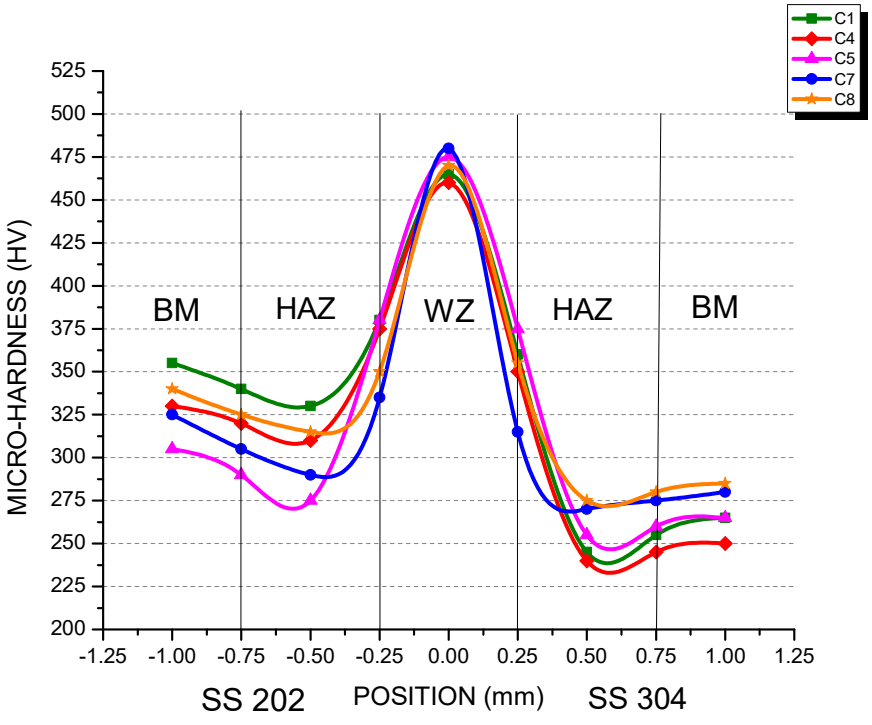

Fig. 18. Micro-Hardness variation with the distance from the weld

5.3 Residual Stress (MPa)

Fig. 19. shows position 3 under the X-ray diffractor. Standard chromium (Cr) material X-ray tube is used having collimator size of 1mm diameter with 30kV and 1mA specification.

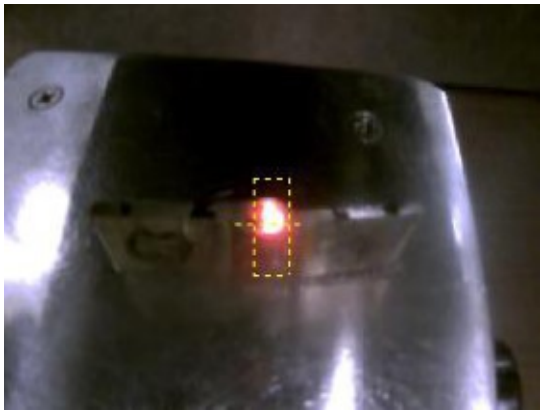

Fig. 19. Sample C7 under X-Ray Diffractor

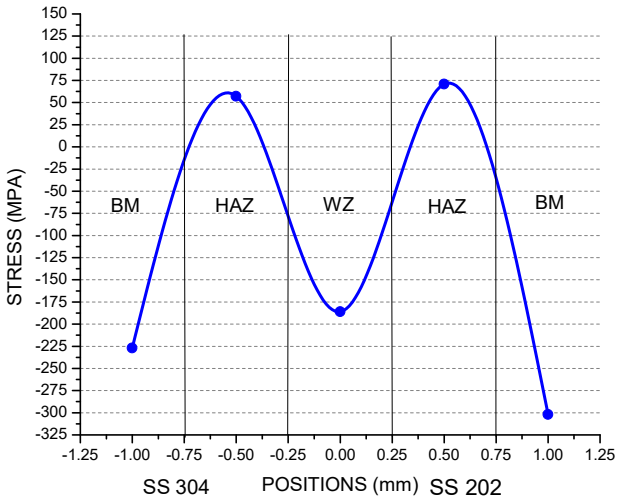

Fig. 20. Residual stress variation at different zones of sample C7 welded at 115 A, 4 mm/s welding speed and 10 % arc length correction factor

Residual stresses are the stresses that are present within a body or a material after the process of manufacturing and material processing in the absence of temperature gradients or external loads [Wan et.al. (2017)].The achieved residual stress values for the C7 welded sample for different regions are as shown in the graph in Fig. 20. Compressive residual stress was produced in the

base plate and weld zone. Tensile residual stress was produced in the heat affected zone (HAZ). During the process of joining by CMT process, due to low heat input, upper and the lower weld zone surfaces experiences a higher rate of solidification due to rapid cooling than the material within the weld pool and the heat-affected zone (HAZ). This uneven rate of cooling leads to differential thermal distribution thus causing expansion in the heat affected zones and contraction in the weld zone. Due to this, the residual stress in the weld zone tends to become negative (compressive) due to shrinkage of the grain size (fine grains). The compressive stress in a way is desirable as it helps in avoiding the formation of cracks and notches. Relief from stress corrosion cracking also observed in the weld region. The slow cooling and coarser grains in the heat-affected zone (HAZ) results in a positive or tensile residual stress. This tensile residual stress present in the heat-affected zone is detrimental and results in fatigue failure. There may be chances of crack initiation and thus material fails most of the time in this region which leads to degradation of mechanical properties. The plots obtained in Fig. 21. for samples C1, C4, C5, C7, C8 between SS 304 and SS 202 was nearly the mirror images of each other. A similar type of results was observed in all the samples.

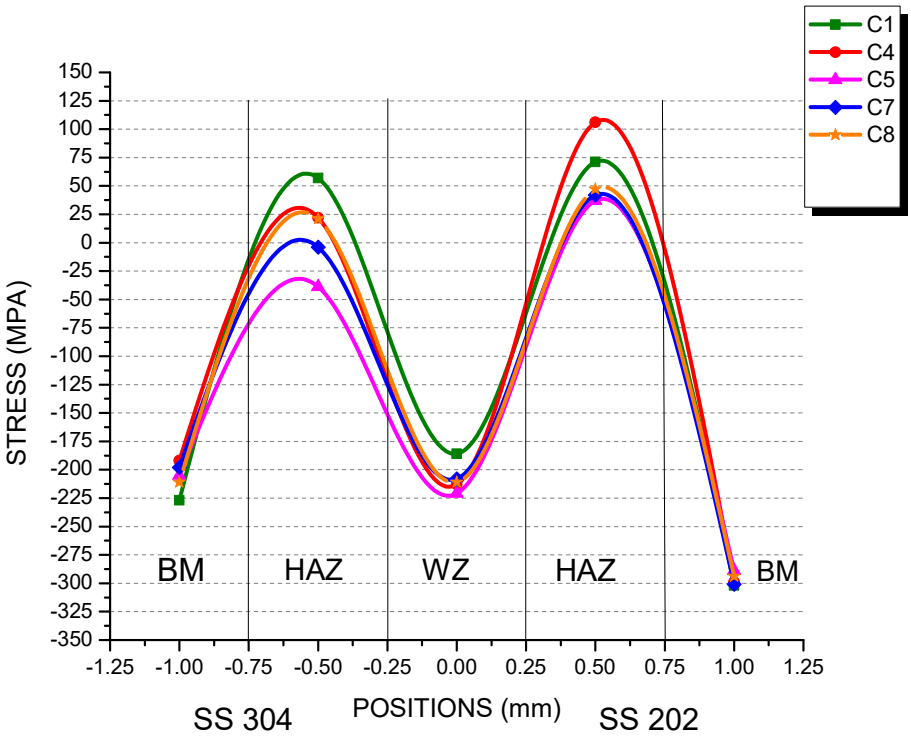

Fig. 21. Residual stress variation at different zones of welded samples

CHAPTER 7: CONCLUSIONS

The paper investigates the mechanical characteristics of welded joints of dissimilar austenitic steels SS202 and SS304 thin sheets by cold metal transfer welding technique. The below mentioned are the conclusions drawn from this experimental study:-

1) CMT welding is a suitable technique for welding thin stainless steel plates of dissimilar grades and different thicknesses.
2) A tailor welded blank of blank ratio 1.67 can be made of stainless steel sheets of grades SS 304 and SS 202 with optimum strength and hardness.
3) The highest strength equal to 291 MPa and highest hardness equal to 480 HV is achieved at 115 A current, 4 mm/s welding speed, and 10 % arc length correction factor.
4) The results obtained by the experimental work is analyzed and it validates the result obtained by Taguchi L9 optimization technique.
5) Low heat input and rapid cooling in CMT welding results in compressive (negative) residual stress in the weld zone making it the strongest and hardest zone.
6) The HAZ is the most affected portion of the joint due to coarser grains and tensile residual stress because of the slow cooling here thus making it a hotspot for failure. The necking starts in the thinner section and results in cup-cone shaped fracture.

REFERENCES

1. Cai M., Wu C. and Gao X. (2018), IOP Conference Series.: Earth and Environmental Science, 170, 042106.
2. Cao R., Wang T., Wang C., Feng Z., Lin Q. and Chen J.H. (2018), Cold metal transfer welding–brazing of pure titanium TA2 to magnesium alloy AZ31B, Journal of Alloys and Compounds, 605, 12-20.
3. Cao R., Yu G., Chen J.H. and Wang P.C. (2013), Cold metal transfer joining aluminum alloys-to-galvanized mild steel, Journal of materials processing technology, 213(10), 1753-1763.
4. Chaudhari R., Parekh R. and Ingle A. (2014), Reliability of dissimilar metal joints using fusion welding: A Review, In International Conference on Machine Learning, Electrical and Mechanical Engineering, (4-5), 1657-1664.
5. Cook G.E. and Eassa H.E.D.E. (1985), The effect of high-frequency pulsing of a welding arc, IEEE Transactions on Industry Applications, 5, 1294-1299.
6. Cui Y., Xu C. and Han Q. (2007), Microstructure improvement in weld metal using ultrasonic vibrations, Adv. Eng. Materials, 7, 161-163.
7. Dai W. (2003), Effects of high-intensity ultrasonic-wave emission on the weldability of aluminum alloy 7075-T6, Mater. Lett., 57, 2447-2454.
8. Darwish S.M. and Samhan A.M. (2004), Thermal stresses in carbide tip bonded face milling cutters, J. Mater. Process. Technol., 147, 51–59.
9. Decroix J.H. (1968), Deformation Under Hot Working Conditions, The Iron and Steel Institute London, P. 315.
10. Dupont J. and Kusko C.S. (2007), Martensite Formation in Austenitic/Ferritic Dissimilar Alloy Welds, Welding Journal, February, 51s-54s.
11. Feng J., Zhang H. and He P. (2009), The CMT short-circuiting metal transfer process and its use in thin aluminium sheets welding, Materials & Design, v. 30, pp. 1850–1852.
12. Fisher T.P. (1973), Effects of vibrational energy on the solidification of aluminum alloys, Br Found, 66:71–84.
13. Form G.W. and Wallace J.F. (1960), Effect of low frequency mechanical vibration on solidifying metals, Trans AFS, 68:145–56.

14. Ghosh N., Pal P.K. and Nandi G. (2017), GMAW dissimilar welding of AISI 409 ferritic stainless steel to AISI 316L austenitic stainless steel by using AISI 308 filler wire, Engineering Science and Technology-an International Journal, 20(4), 1334-1341.
15. Gungor B., Kaluc E., Taban E. and Aydin S.I.K. (2014), Mechanical and microstructural properties of robotic Cold Metal Transfer (CMT) welded 5083-H111 and 6082-T651 aluminum alloys, Materials & Design, 54, 207-211.
16. Gupta A. (2019), Determination of residual stresses for helical compression spring through Debye-Scherrer ring method, Materials Today Proceedings.
17. Hanninen H., Romu J., IIola R., Tervo J. and Laitinen A. (2001), Effects of processing and manufacturing of high nitrogen-containing stainless steels on their mechanical, corrosion and wear properties, J Mater Process Technol, 117:424–30.
18. Hasanbasoglu A. and Kacar R. (2007), Resistance Spot Weldability of Dissimilar Materials (AISI 316L-DIN EN 10130-99 Steels), Material and Design, 28, 1794-1800.
19. Hu S., Zhang H., Wang Z., Liang Y. and Liu Y. (2016), The arc characteristics of cold metal transfer welding with AZ31 magnesium alloy wire, Journal of Manufacturing Processes, 24, 298-306.
20. Ibrahim I.A., Mohamat S.A., Amir A. and Ghalib, A. (2012), The Effect of Gas Metal Arc Welding (GMAW) processes on different welding parameters, Procedia Engineering, 41, 1502-1506.
21. Irizalp A.O., Durmus H., Yuksel N. and Turkmen I. (2016), Cold metal transfer welding of AA1050 aluminum thin sheets, Materia (Rio de Janeiro), 21(3), 615-622.
22. Joseph A., Rai S.K., Jayakumar T. and Murugan N. (2005), Evaluation of residual stresses in dissimilar weld joints, International Journal of Pressure Vessels and Piping, 82, 700–705.
23. Kannan R., Shanmugam N.S. and Naveen S. (2019), Effect of Arc Length Correction on Weld Bead Geometry and Mechanical Properties of AISI 316L Weld ments by Cold Metal Transfer (CMT) Process, 18-3916–3921.
24. Keshari R.K. and Sahu P.L. (2019), Mechanical characterization of dissimilar welded joint of SS202 and SS304 by tungsten inert gas welding , Vol-3, Issue-4, 245-252.

25. Khraisheh M., Abu-Dheir N., Saito K. and Male A. (2004), Effect of mold vibration on the solidification process during gravity die casting of AA356, TMS annual meeting, USA; March, p. 361–72.
26. Kocatepe K. (2007), Effect of low frequency vibration on porosity of LM25 and LM6 alloys, Mater Des, 28(6):1767–75.
27. Kocatepe K. and Burdett C.F. (2000), Effect of low frequency vibration on macro and micro structures of LM6 alloys, J Mater Sci, 35:3327–35.
28. Kou S. (2003), Welding Metallurgy, second ed., John Wiley, Hoboken, New Jersey.
29. Kumar N.P., Vendan S.A. and Shanmugam N.S. (2016), Investigations on the parametric effects of cold metal transfer process on the microstructural aspects in AA6061, J. Alloy Compound, 658, 255-264.
30. Lin J., Ma N., Lei Y. and Murakawa H. (2013), Shear strength of CMT brazed lap joints between aluminum and zinc-coated steel, Journal of materials processing technology, 213(8), 1303-1310.
31. Little R.L. (1994), Welding and welding technology, Tata McGraw Hill, 198-242.
32. Lorenzin G. and Rutili G. (2009), The innovative use of low heat input in welding: experiences on cladding and brazing using the CMT process, Welding International, 23(8), 622-632.
33. Magalhaes R.R., Vieira A.B. Jr. and Barra S.R. (2013), The use of conventional strain gauges evaluation for measurements of residual stresses in welded joints, Journal of the Brazilian Society of Mechanical Sciences and Engineering, 36 (1):173-180.
34. Marashi S.P.H., Pouranvari M., Salehi1 M., Abedi A. and Kaviani S. (2008), Overload failure behaviour of dissimilar thickness resistance spot welds during tensile shear test, Mater. Sci. Eng., A480, 175–180.
35. Mendez P.F. and Eagar T.W. (2001), Welding processes for aeronautics, Advanced materials and processes, 159(5), 39-43.
36. Merkler M. (2004), CMT- The new revolution in digital GMA welding, Fronius International GmbH, Wels.
37. Mishra R.R., Tiwari V.K. and Rajesha S. (2014), A study of tensile strength of MIG and TIG welded dissimilar joints of mild steel and stainless steel, International Journal of Advances in Materials Science and Engineering, 3(2), 23-32.

38. Okumura T. and Taniguchi C. (1982), Engenharia de Soldagem e Aplicacoes, Rio de Janeiro: LTC.
39. Pickin C.G., Williams S.W. and Lunt M. (2011), Characterization of the cold metal transfer (CMT) process and its application for low dilution cladding, Journal of Materials Processing Technology, v. 211, n. 3, pp. 496-502.
40. Pillai R.M., Biju Kumar K.S. and Pai B.C. (2004), A simple inexpensive technique for enhancing density and mechanical properties of Al–Si alloys, J Mater Process Technol, 146:338–48.
41. Prakash A. and Mangal D. (2017), Study And Assessment Of Mechanical Properties Of Resistance Spot Weld Of Two Dissimilar Metals, 6(10) 2277-9655.
42. Ramkumar T., Selvakumar M., Narayanasamy P., Begam A.A., Mathavan P. and Raj A.A. (2017), Studies on the structural property mechanical relationships and corrosion behavior of Inconel 718 and SS 316L dissimilar joints by TIG welding without using activated flux, J Manuf Process, 30:290–8.
43. Sabooni S., Karimzadeh F., Enayati M.H. and Ngan A.H.W. (2015), Friction-stir welding of ultrafine grained austenitic 304L stainless steel produced by martensitic thermomechanical processing, Mater. Des., 76, 130–140.
44. Saghafian H., Yadollah-Tabar H. and Shabestari S. (2006), The effects of low frequency mechanical vibration during solidification on microstructure and mechanical properties of A380 aluminum alloy, MSc dissertation, Iran University of Science and Technology, Iran, [Persian language].
45. Sammaiah P., Suresh A. and Tagore G.R. (2010), Mechanical properties of friction welded 6063 aluminum alloy and austenitic stainless steel, Journal of materials science, 45(20), 5512-21.
46. Sasaki T., Msruyama Y., Ohba H. and Ejiri S. (2013), Two Dimensional Imaging of Debye-Scherrer Ring for Tri-Axial Stress Analysis of Industrial Material, IOP publishing for SISSA Midea Lab, Paris, France.
47. Sathiya P., Aravindan S. and Haq A.N. (2005), Mechanical and metallurgical properties of friction welded AISI 304 austenitic stainless steel, The International Journal of Advanced Manufacturing Technology, 26(5-6), 505-11.

48. Shanmugasundar G., Karthikeyan B., Ponvell P.S. and Vignesh V. (2019), Optimization of Process Parameters in TIG Welded Joints of AISI 304L -Austenitic Stainless Steel using Taguchi's Experimental Design Method, 16, 1188–1195.
49. Sugahara H.J., Barros P.S., Melo L.G., Goncalves I.L., Rolim T.L., Yadava Y.P. and Ferreira R.A. (2018), Measurement of Residual Stresses in Welded Joints by DCP Method, Materials Research, 21(4).
50. Taban E., Gould J.E. and Lippold J.C. (2010), Dissimilar friction welding of 6061-T6 aluminum and AISI 1018 steel: Properties and microstructural characterization, Materials & Design, 31(5), 2305-2311.
51. Totten G.E. and MacKenzie D.S. (2003), Handbook of aluminum, Physical metallurgy and processes, vol. 1. USA: CRC Press.
52. Tseng K. and Lin P.Yu. (2014), UNS S31603 Stainless Steel Tungsten Inert Gas Welds Made with Microparticle and Nanoparticle Oxides, 7, 4755-4772.
53. Tseng M.M. and Hu S.J. (2014), Mass customization in CIRP Encyclopedia of Production Engineering, Springer Berlin Heidelberg, 836-843.
54. Varghese P., Vetrivendan E., Kamaraj M., Ningshen S. and Mudali U.K. (2019), Weld overlay coating of Inconel 617M on type 316L stainless steel by cold metal transfer process, Surf. Coat. Technol., 357 1004–13.
55. Wan Y., Jiang W., Li J., Sun G., Kim D.K. and Woo W. (2017), Weld residual stresses in a thick plate considering back chipping: Neutron diffraction, Contour method and finite element simulation study. Materials Science and Engineering, A 699, 62-70.
56. Wang J., Feng J.C. and Wang Y.X. (2008), Microstructure of Al–Mg dissimilar weld made by cold metal transfer MIG welding, Materials Science and Technology, 24(7), 827-831.
57. Watanabe T., Ookawara S., Seki S. and Yanagisawa A. (2003), The effect of ultrasonic vibration on the mechanical properties of austenitic stainless steel weld. Quart, J. JWS, 21 (2), 249–255.
58. Watanabe T., Shiroki M. and Yanagisawa A. (2010), Improvement of mechanical properties of ferritic stainless steel weld metal by ultrasonic vibration, Journal of Materials Processing Technology, 210, 1646–1651.
59. Williams N.T. and Parker J.D. (2005), Int. Mater. Rev., 49, 45– 75.

60. Withers P.J. and Bhadeshia H.K.D.H. (2001), Residual stress Part 1 - Measurement techniques, Materials Science and Technology, 17(4):355-365.
61. Yan J., Ming G. and Xiaoyan Z. (2010), Study microstructure and mechanical properties of 304 stainless steel joints by TIG, laser and laser-TIG hybrid welding, J Optics and Lasers in Eng 48, 512-517.
62. Yang S., Zhang J., Lian J. and Lei Y. (2013), Welding of aluminum alloy to zinc coated steel by cold metal transfer, Materials & Design, 49, 602-612.
63. Yuan T., Kou S. and Luo Z. (2016), Grain refining by ultrasonic stirring of the weld pool, Acta Materialia, 106, 144-154.
64. Zhang C., Li G., Gao M., Yan J. and Zeng X.Y. (2013), Microstructure and process characterization of laser cold metal transferhybrid welding of AA6061 aluminium alloy, The International Journal of Advanced Manufacturing Technology, 68(5-8), 1253-1260.
65. Zhang H. and Senkara J. (2005), Resistance welding: fundamentals and applications, Boca Raton FL, CRC Press, 196–201.